

Noise spectra of stochastic pulse sequences: Application to large-scale magnetization flips in the finite size two-dimensional Ising model

Zhi Chen and Clare C. Yu

Department of Physics and Astronomy, University of California–Irvine, Irvine, California 92697, USA

(Received 10 March 2009; published 16 April 2009)

We provide a general scheme to predict and derive the contribution to the noise spectrum of a stochastic sequence of pulses from the distribution of pulse parameters. An example is the magnetization noise spectra of a two-dimensional Ising system near its phase transition. At $T \leq T_c$, the low-frequency spectra is dominated by magnetization flips of nearly the entire system. We find that both the predicted and the analytically derived spectra fit those produced from simulations. Subtracting this contribution at T_c leaves the high-frequency spectra which follow a power law determined by the critical exponents.

DOI: [10.1103/PhysRevB.79.144420](https://doi.org/10.1103/PhysRevB.79.144420)

PACS number(s): 05.40.Ca, 73.50.Td, 75.40.Gb, 75.40.Mg

Noise due to random pulses is ubiquitous. Examples include switching the rotational direction of the flagellar motor in *Escherichia coli* bacteria,¹ switching in electrical resistance,² and magnetization of systems near a phase transition.³ Yet another example is crackling noise in which slowly driven systems produce sudden discrete outbursts spanning a broad range of sizes.⁴ Instances of crackling noise include the sound of paper crumpling, Barkhausen noise from domain movement in ferromagnets,^{5,6} flux noise from vortices entering a superconductor as the external magnetic field is increased,⁷ and the seismic activity during earthquakes.⁸

The question is how these pulses are reflected in the features of the power spectra commonly used to characterize noise. The answer could be used to estimate or predict the pulse noise spectrum as well as to separate the pulse contribution to the noise spectrum from other sources. For example, suppose one wants to determine the critical exponents of a second-order phase transition from the noise spectra.^{3,9,10} In a finite size system with a discrete broken symmetry, switching between degenerate ordered phases will also contribute to the noise spectra, and it is important to separate out this contribution before determining the critical exponents.

Previous work calculated the noise from stochastic pulse sequences.^{11–14} Machlup showed that random telegraph noise consisting of square pulses with exponentially distributed durations has a Lorentzian noise spectrum.¹¹ Subsequently others^{12–14} considered a more general pulse shape and distribution, though their theory cannot be applied if the pulse shape depends on the pulse index m , e.g., if the pulses alternate in sign as shown in Fig. 1. In this paper we determine the noise spectrum from a distribution of pulse parameters for a much more general sequence of stochastic pulses with amplitudes that can (but need not) depend on m . As simple examples, we consider square pulse trains which produce a flat low-frequency noise spectrum, and sawtooth signals which produces a bump in the noise spectrum. We then analyze the magnetization noise spectra of a finite size two-dimensional (2D) Ising system near the phase transition. We map the collective jumps (or flips) in the magnetization to a sequence of discrete pulses, and use our algorithm to predict the contribution to the noise using reasonable assumptions

about the distribution of pulse parameters and characteristic frequencies from the noise spectrum. We check this prediction with the spectra found from Monte Carlo simulations. We then check our algorithm by determining the distribution of pulse parameters from the magnetization time series, and derive noise spectra in excellent agreement with that found from Monte Carlo simulations. We find that the low-frequency magnetization noise spectra have a distinct signature due to the global magnetization flips of the whole spin system which is particularly evident below T_c . Subtracting this contribution at T_c yields the high-frequency power-law noise spectrum dictated by the critical exponents of the infinite system.

We now present a general formulation to find the ensemble averaged noise spectrum of a sequence of stochastic pulses $X(t)$ consisting of K pulses. As shown in Fig. 1, each pulse has a duration r with an interval q where the signal is zero between two successive pulses. The maximum height $H(m)$ of the m th pulse has two factors: $H(m) = h \cdot a(m)$, where h is a random variable, and $a(m)$ contains the functional dependence on m . We only consider the case where $a(m) = A^m$, A is a constant, and $0 < |A| \leq 1$. $|A| < 1$ corresponds to a decay envelope. Denote r , h , and q for the m th pulse by r_m , h_m , and q_m , respectively. $X(t)$ can be expressed as

$$X(t) = \sum_{m=1}^K x_m(t - t_m), \quad (1)$$

where the m th pulse is $x_m(t - t_m)$, and $t_m = \sum_{j=1}^{m-1} (r_j + q_j)$, $m \geq 2$ is the corresponding time delay. (The first pulse starts at $t_1 = 0$.) The m th pulse $x_m(t')$ starts at $t' = t - t_m = 0$.

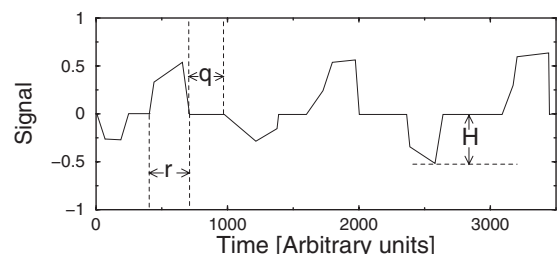


FIG. 1. A representative sequence of stochastic pulses.

We denote the Fourier transform of the pulse $x_m(t')$ by $F_m(\omega, r_m, h_m, q_m)$. Then the Fourier transform $F_X(\omega)$ of Eq. (1) is given by

$$F_X(\omega) = \sum_{m=1}^K F_m(\omega, r_m, h_m, q_m) e^{-i\omega t_m}. \quad (2)$$

$\exp[-i\omega t_m]$ contains the phase relation between pulses. The power spectrum of $X(t)$ is

$$S_X(\omega) = \frac{2}{\tau_K} F_X^*(\omega) F_X(\omega), \quad (3)$$

where $\omega > 0$, and τ_K is the total duration of $X(t)$. $S_X(\omega)$ can be written as

$$\begin{aligned} \tau_K S_X(\omega) = & 2 \sum_{m=1}^K |F_m(\omega, r_m, h_m, q_m)|^2 \\ & + 4 \operatorname{Re} \left[\sum_{m=1}^{K-1} \sum_{n=1}^{K-m} F_n^*(\omega, r_n, h_n, q_n) \right. \\ & \left. \times F_{m+n}(\omega, r_{m+n}, h_{m+n}, q_{m+n}) e^{-i\omega(t_{m+n}-t_n)} \right]. \quad (4) \end{aligned}$$

We assume the following: (a) the values of a pulse's parameters are independent of those of other pulses except for $a(m)$. (b) r, q , and h have the combined distribution $p(r, h, q)$ which is the same for all pulses, and the other pulse parameters (if any) are independent of r, h , and q . Then the ensemble averaged Fourier transform of the pulse $x_m(t')$ is $\iiint drdqdh A^m \bar{F}(\omega, r, h, q) p(r, h, q)$, where ω is the angular frequency, and the overline, e.g., \bar{F} , denotes the average of over parameters other than r, q , and h (e.g., different pulse shapes). (c) $\bar{F}(\omega, r, h, q)$ is independent of the pulse index m .

From assumption (a), F_m/A^m and F_n/A^n , as well as (r_m+q_m) and (r_n+q_n) ($m \neq n$), are uncorrelated. After taking the ensemble average over the pulses and all the parameters, we use assumptions (b) and (c) to obtain

$$\langle \tau_K S_X(\omega) \rangle = 2BI_0 + 4 \operatorname{Re}[AI_2 I_3 R_K], \quad (5)$$

where $\langle \dots \rangle$ is an ensemble average,

$$B = \begin{cases} \frac{|A|^2 - |A|^{2K+2}}{1 - |A|^2}, & \forall |A| < 1 \\ K, & \text{for } |A| = 1. \end{cases} \quad (6)$$

We define

$$R_K = \sum_{m=1}^{K-1} \sum_{n=1}^{K-m} (|A|^2)^n (AI_1)^{m-1},$$

$$I_0(\omega) = \int_{-\infty}^{\infty} dh \int_0^{\infty} \int_0^{\infty} \overline{|F(\omega, r, h, q)|^2} p(r, h, q) drdq,$$

$$I_1(\omega) = \int_{-\infty}^{\infty} dh \int_0^{\infty} \int_0^{\infty} e^{-i\omega(r+q)} p(r, h, q) drdq,$$

$$I_2(\omega) = \int_{-\infty}^{\infty} dh \int_0^{\infty} \int_0^{\infty} \bar{F}(\omega, r, h, q) p(r, h, q) drdq,$$

$$I_3(\omega) = \int_{-\infty}^{\infty} dh \int_0^{\infty} \int_0^{\infty} \bar{F}^*(\omega, r, h, q) e^{-i\omega(r+q)} p(r, h, q) drdq. \quad (7)$$

Doing the sums in R_K yields

$$R_K = \begin{cases} \frac{|A|^2 [1 - (AI_1)^{K-1}]}{(1 - |A|^2)(1 - AI_1)} - \frac{|A|^4 (|A|^{2K-2} - (AI_1)^{K-1})}{(1 - |A|^2)(|A|^2 - AI_1)}, & \forall |A| < 1 \\ \frac{K}{1 - AI_1} - \frac{1 - (AI_1)^K}{(1 - AI_1)^2}, & \text{for } |A| = 1. \end{cases} \quad (8)$$

We define $q' = r + q$ and

$$p_0(q') = \int_{-\infty}^{\infty} dh \int_0^{\infty} p(r, h, q' - r) dr. \quad (9)$$

Then I_1 can be written as

$$I_1 = \int_0^{\infty} e^{-i\omega q'} p_0(q') dq', \quad (10)$$

$$|I_1| < \int_0^{\infty} |e^{-i\omega q'}| p_0(q') dq' = 1, \quad (11)$$

unless

$$p_0(q') = \sum_m b_m \delta(q' - q'_m), \quad (12)$$

where $q'_j - q'_i = 2\pi\ell/\omega$, (i, j , and ℓ are integers), $b_m > 0$ and $\sum_m b_m = 1$.¹⁵ Thus when $K \rightarrow \infty$, the power spectrum for $\omega > 0$ is

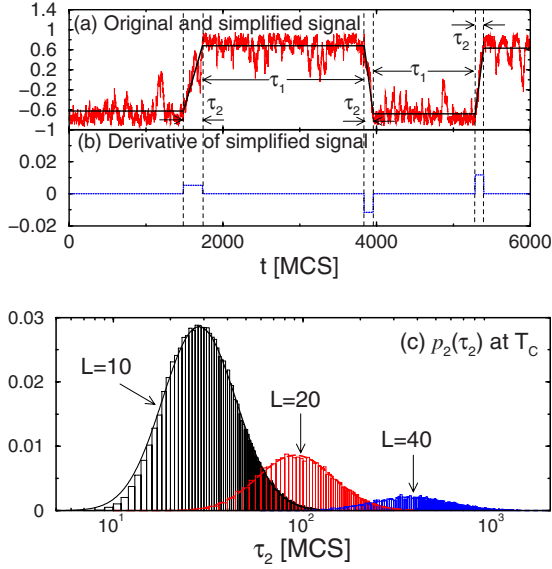


FIG. 2. (Color online) (a) The original and simplified time series (solid lines) of the magnetization for the 2D Ising model ($L=20$) at T_c . (b) The time derivative of the simplified signal shown in (a). (c) Distributions $p_2(\tau_2)$ at T_c for different system sizes. Enveloping lines are $p_2(\tau_2)$ from expression given in the text.

$$\langle S_X(\omega) \rangle = \frac{2C}{\langle r+q \rangle} \left(I_0 + 2 \operatorname{Re} \left[\frac{A I_2 I_3}{1 - A I_1} \right] \right), \quad (13)$$

where $C = |A|^2 / [K(1 - |A|^2)] + o(K^{-1})$ for all $|A| < 1$, and $C=1$ when $|A|=1$.

Equation (13) can be used to calculate the average noise spectrum of any random pulse sequence satisfying our three assumptions. [Fluctuations uncorrelated with the pulses are not contained in Eq. (13).] A pulse spectrum need not be a Lorentzian, e.g., it may have a bump. As examples, we consider three cases of a time series of trapezoidal pulses such as the simplified signal in Fig. 2(a). [Unlike Fig. 2(a), suppose the signal varies between 0 and 1.] These cases illustrate how the duration τ_1 of the flat part of the signal and the rise time τ_2 are reflected in the spectra. In all three cases we find that simulated time series produce spectra that agree with the spectra derived from Eq. (13) as shown in Fig. 3.

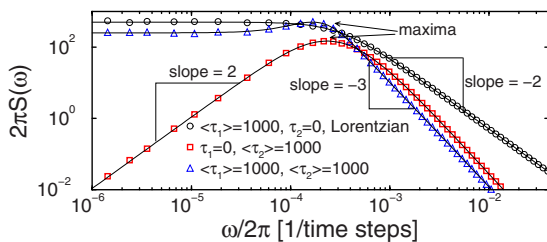


FIG. 3. (Color online) Power spectra of random telegraph noise ($\langle \tau_1 \rangle = 1000, \tau_2 = 0$), random sawtooth noise ($\tau_1 = 0, \langle \tau_2 \rangle = 1000$), and a trapezoidal signal ($\langle \tau_1 \rangle = 1000, \langle \tau_2 \rangle = 1000$). The signals vary between 0 and 1. Nonzero τ_1 and τ_2 are exponentially distributed. Symbols are for spectra averaged over 100 runs, each run having 2^{23} time steps. The solid lines are from Eq. (13) as described in the text.

Example (1) Square Pulses. If $\tau_2=0$ while the pulse duration $r=\tau_1$ and the interval between pulses $q=\tau_1$ have exponential distributions, we have random telegraph noise (two-state switching) with square pulses. We use Eq. (13) to derive the spectrum using $A=1$, the Fourier transform of a square pulse

$$\bar{F}(\omega, r, h, q) = \frac{h}{(i\omega)} (1 - e^{-i\omega r}), \quad (14)$$

the height $h=1$, $p_1(r)=p_1(q)=p_1(\tau_1)$ where

$$p_1(y) = \frac{1}{\langle y \rangle} \exp \left[-\frac{y}{\langle y \rangle} \right], \quad (15)$$

$\langle y \rangle$ is the mean value of y , and $p(r, h, q) = p_1(r)p_1(q)\delta(h-1)$, where $\delta(y)$ is a Dirac delta function. The well-known result is a Lorentzian spectrum (see Fig. 3).¹¹ So the duration τ_1 produces a flat spectrum at frequencies $\omega < (2/\tau_1)$.¹¹

Example (2) Sawtooth Pulses. If $\tau_1=0$ and the rise time τ_2 follows an exponential distribution $p_1(\tau_2)$, then the signal is sawtoothed. In this case we take the time derivative of the signal to obtain positive and negative square pulses with height $h=1/r$ where the square pulse duration r obeys an exponential distribution $p_1(r)=p_1(\tau_2)$. We can use Eq. (13) to derive the spectrum using $A=-1$, Eq. (14) for the Fourier transform of a square pulse, and $p(r, h, q) = 2p_1(r)\delta(q)\delta[h-(1/r)]$. Dividing by ω^2 to undo the derivative, the resulting spectrum shows that the rise time produces a broad bump (see Fig. 3).

Example (3) Trapezoidal Pulses. The pulses are trapezoidal when τ_1 and τ_2 both have an exponential distribution. Again we take the time derivative of the time series to obtain a sequence of square pulses as shown in Fig. 2(b) with the exponential distributions $p_1(q)=p_1(\tau_1)$ and $p_1(r)=p_1(\tau_2)$. We use Eq. (13) to derive the spectrum using $A=-1$, Eq. (14) for the Fourier transform of a square pulse, and $p(r, h, q) = p_1(q)p_1(r)\delta[h-(1/r)]$. We divide the result by ω^2 to undo the derivative. When $\langle \tau_1 \rangle = \langle \tau_2 \rangle$, Fig. 3 shows that the spectrum is flat at low frequencies with a small bump at higher frequencies. It is well known that summing over Lorentzians with different characteristic frequencies yields $1/f$ noise. However, Fig. 3 implies that doing a similar sum over the spectra of trapezoidal pulse sequences with nonzero τ_2 will give $1/f^\alpha$ noise where $\alpha > 1$.

2D Ferromagnetic Ising Model. As a physical example, we now apply Eq. (13) to study the noise spectra of the magnetization M per spin of the 2D Ising model near the phase transition. The Hamiltonian is

$$\mathcal{H} = -J \sum_{i < j} s_i s_j, \quad (16)$$

where the spin $s_i = \pm 1$, (i, j) denotes the nearest-neighbor sites on a square lattice and we set the ferromagnetic exchange $J=1$. In the thermodynamic limit this model has a second-order phase transition at the temperature $T_c = 2.2692/k_B$ (Ref. 16) where k_B is Boltzmann's constant.

We do Metropolis Monte Carlo simulations to obtain the magnetization time series. We apply periodic boundary con-

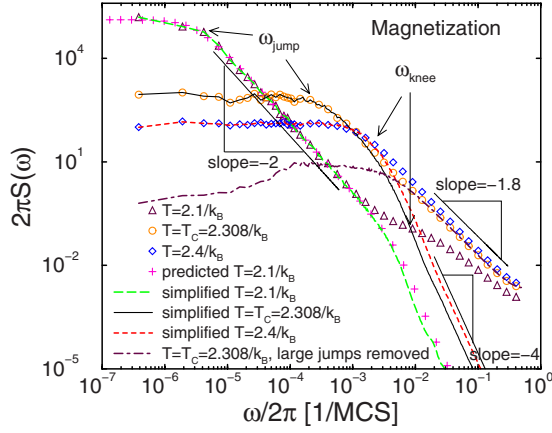


FIG. 4. (Color online) Power spectra of the original (symbols) and simplified (lines) magnetization time series (length $N_K=2\,621\,440$, 10 runs) of the 2D Ising model ($L=20$) at different temperatures.

ditions to a lattice with $N=L^2$ points, where $L=10, 20, 30, 40$. We start each run from a high temperature ($T > T_c$), and then gradually cool the system to $T=0.5 < T_c$. We define T_c for the finite system as the temperature at which the specific heat C_V has a maximum.

At each temperature, we wait until the system equilibrates according to the protocol in Ref. 3. We define the equilibration time Δt_{eq} of the magnetization to be the minimum sampling time needed to obtain an accurate thermodynamic average of the magnetization. To determine Δt_{eq} , we use a block averaging technique^{17,18} in which we divide the magnetization time series into equal segments of length Δt , calculate the susceptibility from the fluctuations in each segment, and then average these values. The average χ and σ_M^2 initially increase as Δt increases, and then plateau at the equilibrium value when $\Delta t \geq \Delta t_{\text{eq}}$.

After the system has reached its equilibration time, we record the magnetization time series for at least 10^6 Monte Carlo time steps per spin (MCS). The noise spectral density $S_x(\omega)$ of a time series $x(t)$ with duration τ_x is normalized so that the total noise power per time step is $S_{\text{tot}} = (1/\tau_x) \sum_{\omega=0}^{\omega_{\text{max}}} S_x(\omega) = \sigma_x^2$, where σ_x^2 is the variance of $x(t)$.³

In Fig. 2(a), we show an example of the magnetization time series at T_c . The noise spectra are shown in Fig. 4. For $T \geq T_c$, starting from high frequencies, we find that the spectra are increasing for decreasing frequencies. However, near a characteristic frequency ω_{knee} , the spectra stop increasing, and at lower frequencies they plateau.

When cooling the system below T_c , the system goes from a disordered paramagnetic phase to an ordered ferromagnetic phase. By spin symmetry, the distribution $P(M)$ of the magnetization per spin is symmetric about $M=0$. So in the ordered phase the system is equally likely to be in either an $M=\tilde{M}$ or $M=-\tilde{M}$ state, where $\pm\tilde{M}$ are the most probable values of M . Thus for a finite size system the magnetization may change from one state to the other and as a result, a jump in the magnetization is created. This is reflected in the noise spectrum. Below T_c the spectrum is similar to the one at T_c for $\omega \geq \omega_{\text{knee}}$. However, as the frequency decreases below ω_{knee} there is a second increase in the spectrum which,

as we shall show, is due to magnetization flips of almost the entire system. In this frequency range ($\omega_{\text{jump}} < \omega < \omega_{\text{knee}}$), $S_M(\omega) \sim \omega^{-2}$ (see Fig. 4). Below the characteristic frequency ω_{jump} , the spectrum plateaus.

We can use our algorithm to predict the contribution of the magnetization flips to the noise spectrum by obtaining values of the distribution parameters directly from the noise spectra. To do this, we start by approximating the time series of these jumps by a trapezoidal signal as shown in Fig. 2(a). τ_1 is the dwell time in the flat region of up or down magnetization, and τ_2 is the duration of the jump. To apply Eq. (13) to obtain noise spectra, we take the time derivative of the simplified signal to obtain a sequence of stochastic square pulses [see Fig. 2(b)]. Thus τ_1 and τ_2 correspond to q and r in Eq. (13).

If there is a constant probability to switch in each time interval, then τ_1 follows an exponential distribution $p_1(\tau_1)$ given by Eq. (15) with mean $\langle \tau_1 \rangle$: $p_1(\tau_1) = p_1(q)$. From the noise spectrum at $T=2.1 < T_c$, we estimate $\langle \tau_1 \rangle \sim 1/\omega_{\text{jump}} \sim 10^5$ MCS.

When the magnetization of the system flips, it overcomes an energy barrier centered at $M=0$ resulting in a bimodal distribution $P(M)$. It takes the magnetization a time τ_2 to execute this flip. To find the distribution $p_2(\tau_2)$, we approximate τ_2 by $\tau_2 \approx t^a + t^b$, where t^a is the time to go from $M=-\tilde{M}$ to $M=0$, and t^b is the time to go from $M=0$ to $M=\tilde{M}$. From spin symmetry, t^a and t^b should follow the same distribution. We can find this distribution from our simulations. In the simulations, the fluctuation of the magnetization between $\pm\tilde{M}$ and 0 is a stochastic process consisting of a series of small steps in magnetization. Each step can increase or decrease the magnetization. The probability that a small step occurs is given by the Boltzmann probability $\exp(-\beta\Delta E)$, where ΔE is the change in energy associated with the change in magnetization. From our simulations we find that t^a and t^b obey a log-normal distribution given by

$$p'_2(z) = \left(\frac{1}{z\sqrt{2\pi\sigma^2}} \right) \exp \left[-\frac{(\ln z - \rho)^2}{2\sigma^2} \right], \quad (17)$$

where $z=t^a$ or t^b . ρ and σ are determined from the mean of τ_2 given by

$$\langle \tau_2 \rangle = 2 \exp \left[\rho + \left(\frac{\sigma^2}{2} \right) \right] \quad (18)$$

and the variance of τ_2 given by

$$\sigma_{\tau_2}^2 = 2(\exp[2\rho + 2\sigma^2] - \langle \tau_2 \rangle^2). \quad (19)$$

Since $\tau_2 = r = t^a + t^b$, the distribution $p_2(r) = p_2(\tau_2)$ is given by the convolution $p_2(\tau_2) = \int dy p'_2(y) p'_2(\tau_2 - y)$. From the $T=2.1$ noise spectrum, we estimate $\langle \tau_2 \rangle \sim 1/\omega_{\text{knee}} \sim 100$, and $\sigma_{\tau_2} \sim \langle \tau_2 \rangle / 2 \sim 50$.

Now we can apply Eq. (13) to analyze the magnetization of the 2D Ising model. For the derivative [Fig. 2(b)] of the simplified magnetization series, $A=-1$, the Fourier transform of a square pulse is given by Eq. (14), and q is independent of r . We assume $h=1.3/\tau_2$. Thus the combined distribution becomes $p(r, h, q) = p_1(q) p_2(r) \delta(h - 1.3/\tau_2)$. Doing the inte-

grals in Eq. (7) numerically, and dividing the result of Eq. (13) by ω^2 to undo the derivative, we obtain the spectra shown in Fig. 4 which is a good approximation at low frequencies. Thus we predict that pulses dominate the low-frequency spectrum.

We can check this prediction by extracting a simplified trapezoidal signal that represents a series of magnetization jumps as shown in Fig. 2(a). In the flat regions with small fluctuations, we replace the original magnetization time series by the mean magnetization in that region. To find the jumps, we start from points with $M=0$, then move both forward and backward in time. A jump is identified if and only if M in one direction achieves $\tilde{M}-\delta M$, and in the other direction achieves $-\tilde{M}+\delta M$, where $\delta M > 0$ is the offset. In Fig. 4, for $T < T_c$, we find that the spectra of the original and simplified magnetization series match at low frequencies ($\omega \ll \omega_{\text{knee}}$). At T_c up to frequencies 1 order of magnitude higher than the crossover frequency, the power spectrum for the simplified signal fits the spectrum of the original signal very well. This is why this contribution must be subtracted from the spectrum before extracting the high-frequency power law dictated by the critical exponents. In Fig. 4 the high-frequency noise at T_c follows $S(\omega > \omega_{\text{knee}}) \sim \omega^{-\mu_M}$ where $\mu_M = 1.8$. This matches well with the scaling theory prediction:^{3,9,10} $\mu_M = 1 + \gamma/(z\nu) = 1.8$, where z is the dynamic critical exponent for the relaxation time $\tau \sim \xi^z$, ν is the critical exponent for the divergence of the correlation length $\xi \sim \varepsilon^{-\nu}$, γ is the critical exponent for the divergence of the magnetic susceptibility $\chi \sim \varepsilon^{-\gamma}$, and $\varepsilon = |(T/T_c) - 1|$ is the reduced temperature.

From the simplified time series, we can extract the parameters for the pulse distributions to derive the pulse contribution to the noise spectra by using Eq. (13) in the same way as we did for the estimate. We use $h = C(T)/\tau_2$ where $C(T)$ is a function of the temperature T . We use the same distributions

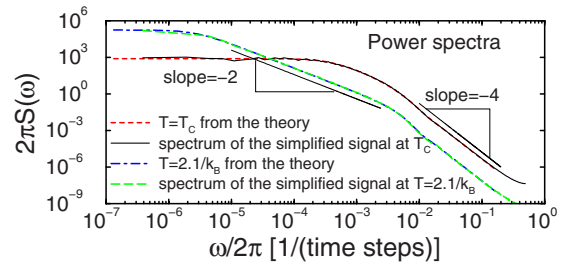


FIG. 5. (Color online) Power spectra for the magnetization jumps of the simplified magnetization signal at $T=T_c$ and $T=(2.1/k_B) < T_c$ for $L=20$. At T_c , $\langle \tau_1 \rangle = 1030.7$, $\langle \tau_2 \rangle = 127.3$, $\sigma_{\tau_2}^2 = 3942.7$. At $T=2.1/k_B$, $\langle \tau_1 \rangle = 1.169 \cdot 10^5$, $\langle \tau_2 \rangle = 115.1$, $\sigma_{\tau_2}^2 = 1718.3$.

for τ_1 and τ_2 , and obtain values for $\langle \tau_1 \rangle$, $\langle \tau_2 \rangle$, and $\sigma_{\tau_2}^2$ from the simplified time series. As shown in Fig. 2(c), $p_2(\tau_2)$ fits very well with the actual distribution of τ_2 for different system sizes. We obtain the spectra shown in Fig. 5 which is an excellent fit to the spectra of the simplified magnetization signals for $T \leq T_c$. The square-wave-like time series of the derivative of the simplified signal [Fig. 2(b)] yields a power spectrum similar to that of a Lorentzian. Undoing the derivative with a factor of $1/\omega^2$ yields a high-frequency noise spectrum that goes as $1/\omega^4$.

In summary, our method predicts and derives the noise spectra of stochastic pulse sequences from the distribution of pulse parameters. It can be used to separate out the contribution of pulses from other contributions to the spectra. This general approach can be applied to a wide variety of phenomena such as switching¹⁻³ and crackling noise.⁴⁻⁸ It can even be used for noise spectra not derived from a time series.

This work was supported by DOE Grant No. DE-FG02-04ER46107.

¹E. Korobkova *et al.*, Nature (London) **428**, 574 (2004); Y. Tu and G. Grinstein, Phys. Rev. Lett. **94**, 208101 (2005); E. A. Korobkova, T. Emonet, H. Park, and P. Cluzel, *ibid.* **96**, 058105 (2006).
²M. B. Weissman, Rev. Mod. Phys. **60**, 537 (1988) and references therein.
³Z. Chen and C. C. Yu, Phys. Rev. Lett. **98**, 057204 (2007).
⁴J. P. Sethna, K. A. Dahmen, and C. R. Myers, Nature (London) **410**, 242 (2001).
⁵M. Celasco, F. Fiorillo, and P. Mazzetti, Nuovo Cim., B **23**, 376 (1974).
⁶S. Zapperi, C. Castellano, F. Colaiori, and G. Durin, Nat. Phys. **1**, 46 (2005).
⁷S. Field, J. Witt, F. Nori, and X. Ling, Phys. Rev. Lett. **74**, 1206 (1995).
⁸H. Houston, H. M. Benz, and J. E. Vidale, J. Geophys. Res. **103**, 29895 (1998).

⁹J. C. Angles d'Auriac, R. Maynard, and R. Rammal, J. Stat. Phys. **28**, 307 (1982).
¹⁰K. B. Lauritsen and H. C. Fogedby, J. Stat. Phys. **72**, 189 (1993); K. Leung, J. Phys. A **26**, 6691 (1993).
¹¹S. Machlup, J. Appl. Phys. **25**, 341 (1954).
¹²T. Lukes, Proc. Phys. Soc. **78**, 153 (1961).
¹³C. Heiden, Phys. Rev. **188**, 319 (1969).
¹⁴M. Celasco and A. Stepanescu, J. Appl. Phys. **48**, 3635 (1977) and references therein.
¹⁵P. Mazzetti and G. P. Soardo, IEEE Trans. Inf. Theory **13**, 552 (1967).
¹⁶K. Huang, *Statistical Mechanics*, 2nd ed. (John Wiley & Sons, Inc., New York, 1987).
¹⁷C. C. Yu and H. M. Carruzzo, Phys. Rev. E **69**, 051201 (2004).
¹⁸A. M. Ferrenberg, D. P. Landau, and K. Binder, J. Stat. Phys. **63**, 867 (1991).